Geotextiles and Geomembranes 52 (2024) 1240–1250

Contents lists available at ScienceDirect

Geotextiles and Geomembranes

journal homepage: www.elsevier.com/locate/geotexmem

Regular Paper

Research on the aging mechanism of polypropylene nonwoven geotextiles under simulated heavy metal aging scenarios

Yuqi Peng [a,b], Zongqiang Zhu [a,b,c,*], Jun Zhang [a,b], Yinian Zhu [a,b], Lihao Zhang [a,b], Yinming Fan [a,b], Xiaobin Zhou [a,b], Shen Tang [a,b], Yusheng Lu [a,b], Wenqian Li [a,b], Yifan Xin [a,b]

[a] Collaborative Innovation Center for Water Pollution Control and Water Safety in Karst Area, Guilin University of Technology, Guilin, 541004, China
[b] The Guangxi Key Laboratory of Theory and Technology for Environmental Pollution Control, Guilin University of Technology, Guilin, 541004, China
[c] Technical Innovation Center of Mine Geological Environmental Restoration Engineering in Southern Karst Area, Nanning, 530022, China

ARTICLE INFO

Keywords:
Polypropylene (PP)
Nonwoven geotextiles
Aging mechanism
Heavy metals
Microplastics

ABSTRACT

We conducted accelerated aging experiments on two types of polypropylene (PP) nonwoven geotextiles (filament geotextile and staple fiber geotextile), immersing them in five different simulated liquids at temperatures of 25 °C, 55 °C, and 85 °C for 200 days. At 85 °C and a pH of 1, the tensile strength and elongation at break of PP filament materials decreased by 95% and 86%, respectively. The presence of heavy metals(arsenic and cadmium), speeds up the aging process in both types of PP geotextiles. Under identical conditions, these heavy metals can increase the loss of tensile strength in geotextiles by more than 7% in 200 days. Increases in temperature, acidic environment, and heavy metal concentration all contribute to faster aging of these geotextiles. Although filament geotextiles exhibit higher tensile strength and elongation at break, staple fiber geotextiles show a lower rate of tensile strength loss during aging and better maintain their tensile strength in high-temperature acidic conditions. During the aging process, cross-linking and recrystallization occur, both of which control the aging rate and the formation of microplastics.

1. Introduction

Geotextiles are products made of polymeric material that is widely used in geotechnical engineering(Carneiro et al., 2023; Santos et al., 2014). Ex-situ solidification/stabilization is a common method for treating heavy metal pollution in soil(Ding et al., 2021; Scanferla et al., 2023; Zhou et al., 2022). In this process, using anti-seepage geotechnical material for risk control is crucial to the technology's success. Nonwoven geotextiles play an important role in controlling these risks and erosion control as a drainage or protective layer(Carneiro et al., 2014; Sprague and Sprague, 2016).

Nonwoven geotextiles inevitably deteriorate during long-term use, a process that is influenced by a combination of environmental factors. Current research has investigated the aging characteristics of polypropylene geotextiles under conditions such as high temperature (Karademir and Frost, 2014, 2021), ultraviolet radiation(Carneiro et al., 2019), natural weathering(Carneiro and Lopes, 2017; Guimarães et al., 2017), and artificial aging scenarios(Carneiro et al., 2014; Scholz et al., 2024). The aging behavior of geotextiles during weathering was found to be highly dependent on their chemical composition(Carneiro and Lopes, 2017). The surface morphology of the geotextile is altered(Jaswal and Vivek, 2023a; Vivek and Dutta, 2022; Vivek et al., 2022b), and the tensile strength and durability of the geotextile are increased(Jaswal et al., 2022; Vivek et al., 2022a) by means of chemical treatments to achieve the purpose of enhancing the shear properties such as geotextile-soil interfaces and improving the strength of the geotextile in engineering reinforcement(Araújo et al., 2022; Jaswal and Vivek, 2023; Vivek et al., 2019). In the production process adding the chemical composition and its ratio is the key to affecting the aging of polypropylene(Carneiro et al., 2023; Nisar et al., 2023). The fabric structure exerts an influence on the in-plane and through-plane hydraulic properties of nonwoven geotextiles(Eskandarnia and Soltani, 2023). There are two main types of nonwoven geotextiles: synthetic staple fiber needle-punched nonwoven geotextiles and synthetic filament spunbond and needle-punched nonwoven geotextiles(Xu et al., 2021). Therefore, the effect of different production processes leading to the aging rate of geotextiles also needs to be studied.

Numerous scholars have investigated the aging behavior of

* Corresponding author. College of Environmental Science and Engineering, Guilin University of Technology, Jiangan Road 12, Guilin, Guangxi, 541004, China.
E-mail address: zhuzongqiang@glut.edu.cn (Z. Zhu).

https://doi.org/10.1016/j.geotexmem.2024.08.006
Received 20 May 2024; Received in revised form 9 August 2024; Accepted 21 August 2024
Available online 27 August 2024

polypropylene geotextiles in different environments, such as landfills (Long et al., 2018; Tollner et al., 2011), marine environments(Carneiro et al., 2018; Philipp et al., 2021), and geotextiles with different treatments under cyclic loading on unpaved roads(Vivek, 2023; Vivek, 2024; Vivek et al., 2022c). Osawa pointed out that metals can catalyze the oxidative degradation of polypropylene (Osawa and Ishizuka, 1973). However, the aging effects of PP materials during accelerated aging in heavy metal (As, Cd) environments are still unclear.

However, most of the studies on the aging process of various geotextiles have focused on the effects of single factors that may accelerate the aging process of the geotextiles through different mechanisms. Annealing and recrystallization of materials are also the keys to controlling the aging of polymeric material(Abdelaal et al., 2015; Ewais and Rowe, 2014). Ewais found that the annealing during the aging of polymeric material increased the strength of the interlayer connection(Ewais and Rowe, 2014). Through differential scanning calorimetry (DSC) and density measurement, it was found that accelerated aging causes the recrystallization of PP material(Dudic et al., 2000). However, the effects and influencing factors of the recrystallization in PP geotextiles during accelerated aging in the presence of heavy metals are not clear.

It is worth noting that geotextiles aging is not only characterized by a gradual degradation of material properties but may also be accompanied by the release of microplastics. Studies on the behavior of polypropylene geotextiles under artificial aging conditions have identified the risk that PP geotextiles may lead to the formation of microplastic particles(Scholz et al., 2024). There is considerable evidence that polypropylene materials degrade and produce microplastics during aging (Browne et al., 2007; Kurniawan et al., 2021; Meides et al., 2022; Thompson et al., 2004). Yang Yu et al. believe that hydrothermal treatment leads to the formation of micro holes on the surface of microplastics(Yu et al., 2024). Many scholars have studied the degradation, accumulation, and toxicology of microplastics (Bhattacharya et al., 2010; Xu et al., 2024; Yu et al., 2024). However, the formation process of microplastics in polypropylene geotextiles under soil heavy metal environments has not been explored.

In summary, to address the aging problem of geotextiles in heavy metal-contaminated site remediation projects, this study aims to fill the gap in the aging characteristics and mechanisms of PP filament geotextiles and PP staple fiber geotextiles under simulated heavy metal aging scenarios.

This study investigates the aging characteristics and mechanisms of PP filament geotextiles and PP staple fiber geotextiles when exposed to different pH, temperature and heavy metal conditions. Specifically, this study will make use of mechanical property tests, differential scanning calorimetry (DSC) and scanning electron microscopy (SEM) to comprehensively assess the changes in properties and microstructural evolution of the materials during the aging process, with a special focus on the release patterns of microplastics and their potential environmental impacts. Through this study, we expect to provide a scientific basis for the selection, use and maintenance of geotextiles in the remediation of heavy metal-contaminated sites, so as to optimize the risk management strategy and ensure the long-term effectiveness of the remediation effect.

2. Materials and methods

2.1. Experimental design

The aging characteristics of two types of polypropylene (PP) nonwoven geotextiles were studied under various conditions. These included different pH levels (1, 6, 8, 13) and a heavy metal solution (pH 6 with arsenic at 1.0 mg/L and cadmium at 4.0 mg/L) at temperatures of 25 °C, 55 °C, 85 °C using double-sided impregnation method. The duration of aging test is 200 days. The concentration of the simulated liquid refers to a heavy metal contaminated site in Liucheng County, Liuzhou City, Guangxi Province. The performance and stability of these geosynthetics were evaluated by examining changes in mechanical properties, microplastic formation, functional group alterations, surface damage and crystallinity, with testing conducted every 40 days. May differ from other similar studies due to the different manufacturers of the experimental equipment used.

2.2. Experimental materials

PP filament geotextiles(Polypropylene filament spunbond and needle-punched nonwoven geotextile, 400 g/m^2) were purchased from Beijing GeoEnviron Engineering & Technology, Inc. Similarly, PP staple fiber geotextiles(Polypropylene staple fiber needle-punched nonwoven geotextile, 400 g/m^2) were obtained from Shandong Luyida New Material Co., Ltd. The mass per unit area of the geotextiles is based on ASTM D5261-10(ASTM D5261-10, 2010).

2.3. Tensile strength test

The tensile tests were carried out using a Universal Testing Machine (UTM). A tension test was conducted on all the tested geotextiles, according to ASTM D4595-17(ASTM D4595-17, 2017). Five specimens of each geotextiles type were tested. Similar numbers of samples were used in previous studies(Vivek et al., 2020). The test settings were: tensile speed of 100 mm/min, spacing length of 100 mm, and clamping distance of 50 mm. Geotextiles were conditioned in a standard environmental state (20 °C ± 2 °C, 60% ± 10% relative humidity) to account for water absorption before testing. Inconsistent moisture content of materials may affect experimental results. Measure the tensile strength(MPa) and then calculate the elongation at break(%).

2.4. Scanning electron microscopy (SEM)

A JSM-7900F scanning electron microscope (Japan Electronics Co., Ltd.) equipped with an energy dispersive spectrometer was used to observe the morphology of the anti-seepage material before and after the experiment. The surface of the sample was sprayed with gold using an ion sputtering coater (JEC-3000FC, Japan Electronics Co., Ltd.) to enhance its conductivity. The scanning voltage was set at 2.0 kV and the magnification levels are 400, 500, and 2000 times.

2.5. FTIR analysis

The anti-seepage geosynthetics were analyzed both before and after the experiment using a 470 FT-IR infrared spectrometer (Thermo Fisher Nicolet) to assess changes in the surface functional groups. Crush the geotextiles through a 100 mesh sieve. The samples were prepared using KBr, and the Attenuation and Total Reflection (ATR) mode was used to determine their chemical compositions (De Carvalho et al., 2024). The infrared spectrum scanning covered a range from 400 to 4000 cm^{-1}. Both background and sample scanning were performed 32 times each. The settings used included a resolution of 4.000, a sampling gain of 1.0, a moving mirror speed of 0.4747, an aperture of 100.00, and a spectral resolution of 1 cm^{-1}.

2.6. DSC measurements

A differential scanning calorimeter (CDR-34P, Cany Precision Instruments Co., Ltd.) was used for the analysis. First, a 10.00 mg sample was weighed and placed under a nitrogen atmosphere with a flow rate of 50 mL/min. The sample was washed for 5 min, then heated to 300 °C at a rate of 10 °C/min, and held at this temperature for another 5 min (Fujiyama et al., 1988). The crystallization melting curve was recorded during this process. Melting enthalpy was determined by integrating the melting curve, and the crystallinity (X_c) was calculated according to the Avrami-Erofeev formula: $X_c = \Delta H_m / \Delta H_m^0$.

where, ΔH_m represents the melting heat of the sample and ΔH_m^0 represents the melting heat of complete crystallization of the sample.

2.7. Micro plastic detection

To detect microplastics, the study used a simulated solution that had soaked the geotextiles as the sample. Stainless steel sieves with different specifications (4 mesh, 16 mesh, 50 mesh and 100 mesh) were employed to transfer and sieve the sample. The larger 4 mesh and 16 mesh sieves helped to intercept big particles and prevent clogging. Minimal deionized water was used to move all material from the 50 mesh and 100 mesh sieves into a clearly marked beaker. The sample was then filtered using a glass sand core filter fitted with a nitrocellulose mesh filter membrane (0.45 μm in pore size, 47 mm in diameter). After initial filtration, the process continued for an additional 5 min to dry the filter membrane thoroughly. Subsequently, the filter membrane was transferred to a marked glass Petri dish. The Petri dish containing the filter membrane was then dried at 35 °C for 24 h before the microplastics were counted and measured.

3. Results and discussion

3.1. Mechanical properties

3.1.1. The effects of pH

PP nonwoven geotextiles are mainly divided into two categories of polypropylene staple fiber needle-punched nonwoven geotextiles and polypropylene filament spunbond and needle-punched nonwoven geotextiles(Xu et al., 2021). Their production processes are staple fiber needle-punched process and filament spunbond and needle-punched process.

Staple fiber needle-punched process is the first carding machine will be made of polypropylene staple fibers into a short-fiber network, interspersed with stacked, or directly by the airflow into the network into a random arrangement of fibers into the fiber network, and then strengthened by the needling process, so that the fibers are intersected with each other entangled in the formation of polypropylene staple fiber needle-punched nonwoven geotextiles.

Filament spunbond and needle-punched method is the first PP slices by heating, extrusion melt into a melt, and then sprayed by the spinneret, cooled by the cooling device, through the airflow stretching or mechanical stretching into a large number of fine filaments, and then chaotically placed in the formation of network curtains to form a fiber mesh, and then through the needle-punched process will be solidified into cloth, the formation of PP filament spunbond and needle-punched nonwoven geotextiles.

Due to the difference between the above two production processes, filament geotextiles fiber length is longer, resulting in filament geotextiles tending to have higher tensile and filtration properties. Due to its unique structural properties, filament geotextiles will have a greater tensile strength impact than staple fiber geotextiles caused by fiber damage at breakage, mainly due to the ability of filament yarns to transmit forces more uniformly, whereas staple fiber geotextiles may have a more complex stress distribution.

Fig. 1 shows how the mechanical properties of PP filament geotextiles change with environmental pH after aging in immersion at temperatures of 55 °C and 85 °C for 200 days. After this period, the tensile strength and elongation at break of the geotextiles in aqueous solutions with pH levels of 6, 8, and 13 are slightly lower than the original values (20.62 MPa, 63%) after 200 days of aging at both temperatures. Generally, aging makes the material more brittle, likely due to the slow depletion of antioxidants, which suggests that it can withstand neutral and alkaline conditions to some extent (Hsuan and Koerner, 1998; Karlsson et al., 1992; Rowe et al., 2010). However, at a pH of 1, the tensile strength significantly drops by 17.60% at 55 °C and by 95.49% at 85 °C, and elongation at break decreases by 5.75% at 55 °C and 86.00% at 85 °C. This indicates that the PP filament geotextiles deteriorates quickly under these conditions, particularly at 85 °C. This rapid aging could be due to the formation of active free radicals from carbon chain fractures, which leads to branching of the polymer chains. Additionally, the presence of H^+ ions may accelerate the material's degradation. The thermal-oxidative aging products of PP might in turn affect the stability of PP(Sedlář and Pác, 1974). It has been found that acetic acid has an accelerating effect on the thermal oxidation of PP (Zhang et al., 2021). In addition, acidic environments and thermal oxidation can synergistically accelerate PP aging in some environments. José et al. discovered that immersion in iron nitrate(pH = 2) and thermo-oxidation have a synergistic effect on the aging of PP geotextiles (Carneiro et al., 2014). This is similar to the results of this experiment.

Fig. 2 depicts how the mechanical properties of PP staple fiber geotextiles change with environmental pH at temperatures of 55 °C and 85 °C over a period of 200 days. The material generally maintains good mechanical properties, although the rates of decline vary under different environmental conditions. After 200 days, the mechanical properties of the PP staple fiber geotextiles at 55 °C are nearly the same as the initial values (16.67 MPa, 78.86%). At 85 °C, the tensile strength and elongation at break remained mostly unchanged under the aging conditions of pH = 1, pH = 6, and pH = 8. However, at pH = 13, the tensile strength dropped from 16.67 MPa to 15.34 MPa, and the elongation at break reduced from 78.86% to 68.07%. This indicates that the PP staple fiber

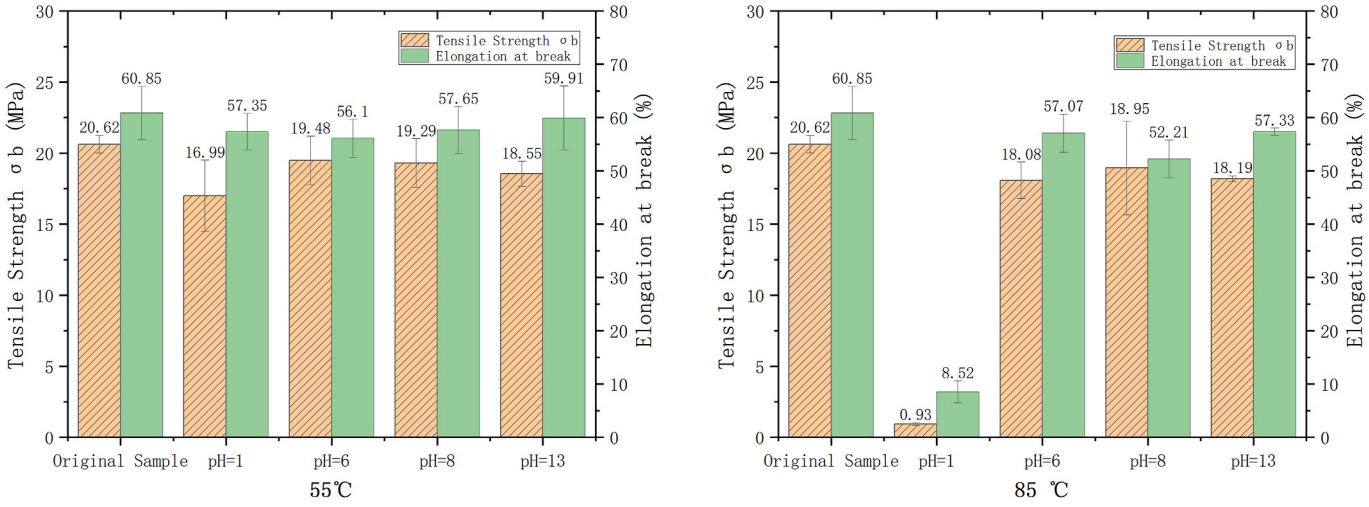

Fig. 1. Effect of pH on the mechanical properties of PP filament geotextile.

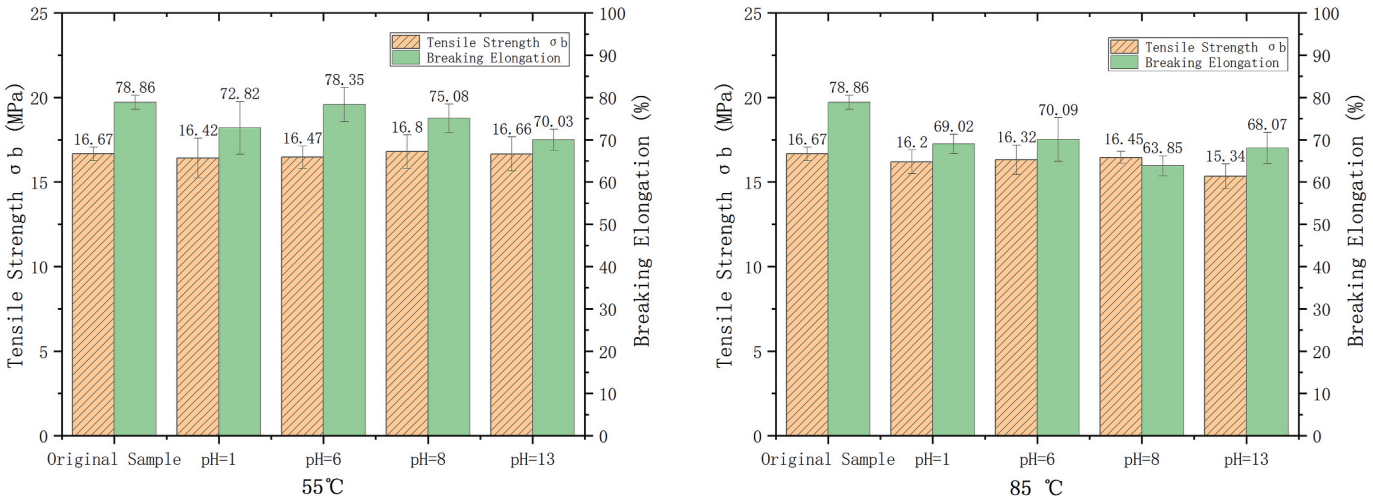

Fig. 2. Effect of pH on the mechanical properties of PP staple fiber geotextile.

geotextiles can retain its mechanical properties in strong acid and neutral environments. Nevertheless, at pH = 13, the material shows signs of degradation, likely due to the combined effects of OH^- ions and water, which result in diminished mechanical properties. José et al. discovered that immersion in sodium hydroxide and thermo-oxidation (90 °C) have a synergistic effect on the aging of PP geotextiles(Carneiro et al., 2014), which is somewhat similar to the results of this study.

In engineering applications we should reduce the synergistic effect of acidity and high temperatures in order to prolong the service life of the geotextiles. On the other hand, we can also be true to the needs of different projects, comprehensive consideration of the choice of appropriate production process of geotextiles.

3.1.2. *Effect of temperature*

Fig. 3 demonstrates how temperature impacts the aging of PP filament geotextiles over 200 days under different environmental conditions, showing a noticeable variation with temperature. In environments with pH levels of 8 (aqueous solution), 13 (aqueous solution), and 6 (heavy metal solution), the overall mechanical properties of the material gradually decline as the temperature increases. Specifically, the tensile strength drops to 18.95 MPa, 18.20 MPa, and 17.96 MPa, respectively, from an initial value of 20.62 MPa, while the elongation at break decreases to 52.2%, 57.3%, and 56.4%, respectively, from the original value of 60.9%. Under pH = 1 (aqueous solution), after 200 days, the tensile strength decreases to 19.36 MPa at 25 °C, 16.99 MPa at 55 °C, and 0.94 MPa at 85 °C. The elongation at break slightly increases to 62.52% at 25 °C but drops to 57.4% at 55 °C and plummets to 8.5% at 85 °C.

The PP filament geotextiles in neutral, alkaline, and heavy metal solution environments show a modest decline in mechanical properties with temperature increasing, yet it manages to maintain a respectable mechanical characteristic. Liu's work suggested that small molecular acids can catalyze the photooxidation of polypropylene(Liu et al., 2020). Under acidic conditions, the presence of H^+ significantly speeds up the degradation of materials, with the rate of reaction escalating as the temperature rises(Hsuan et al., 2005). Additionally, it has been demonstrated that the combined effect of acid and high temperature is more destructive than either factor alone(Carneiro et al., 2014).

Fig. 4 tracks the changes in mechanical properties of PP staple fiber geotextiles over 200 days under varying environmental conditions influenced by temperature changes. In environments with pH levels of 1 (aqueous solution) and 8 (aqueous solution), the data show that upon aging at 25 °C, 55 °C, and 85 °C, the tensile strength first increases then decreases compared to the original value of 16.67 MPa. Moreover, the elongation at break remains around 72.0%, suggesting the potential occurrence of an "Annealing Effect" at 55 °C during the 200-day aging period. This effect likely results from the reintegration of molecular chains and an increase in intermolecular bond energy, which enhances the surface tension and overall mechanical properties of the material (Ferrer-Balas et al., 2001). Conversely, under conditions of pH = 13 (aqueous solution) and pH = 6 (heavy metal solution), the mechanical properties tend to decline with increasing temperature. The tensile

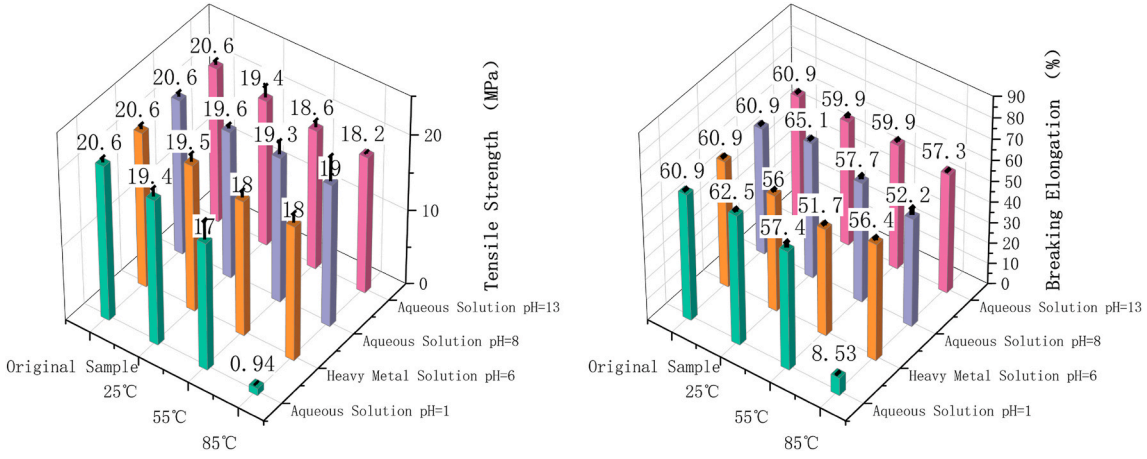

Fig. 3. Effect of temperature on mechanical properties of PP filament geotextile.

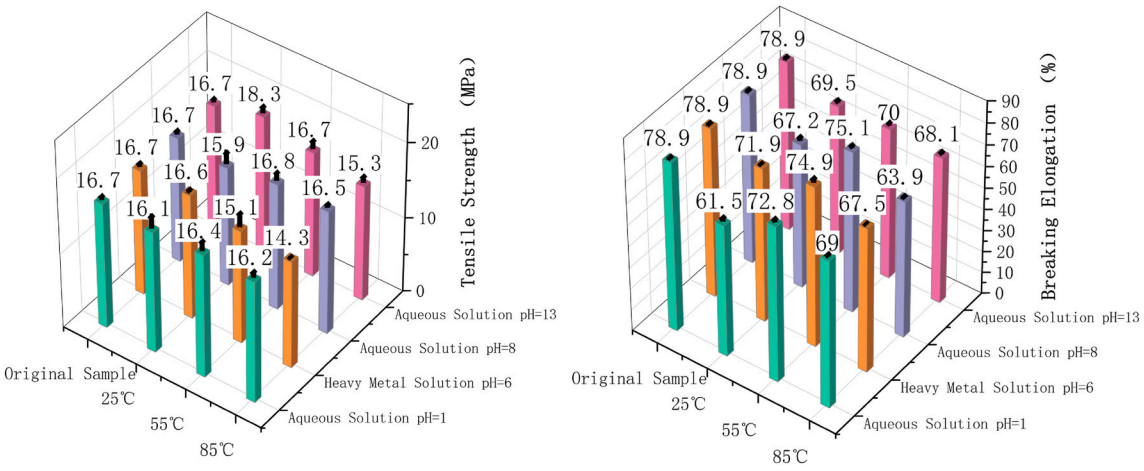

Fig. 4. Effect of temperature on mechanical properties of PP staple fiber geotextile.

strength decreases from the original 16.67 MPa–15.34 MPa and 14.29 MPa, respectively, while the elongation at break drops from 78.9% to 68.1% and 67.5%. This downward trend is attributed to the catalytic effects of OH^- and heavy metals, which accelerate the aging process (Ji et al., 2016; Osawa and Ishizuka, 1973), with heavy metals having a more pronounced impact as shown in the following reaction:

$$2POOH \cdot \xrightarrow{W} PO_2 \cdot + PO \cdot + H_2O$$

here, W represents heavy metals and OH^- ions.

In conclusion, the PP staple fiber geotextiles exhibits minimal change with temperature in acidic and neutral environments, whereas in alkaline and heavy metal-rich conditions, aging intensifies with an increase in temperature.

3.1.3. *Effect of heavy metal concentration*

Polypropylene (PP) undergoes thermo-oxidative reactions when exposed to high temperatures, similar to photo-oxidative reactions. This process involves PP molecules absorbing heat energy, transitioning from a ground state to an excited state, and reacting with oxygen. The presence of heavy metal ions (M^{n+}) acts as a catalyst, speeding up these reactions (Gulec et al., 2004; Ji et al., 2016; Liu and Yang, 2020).

Fig. 5 shows how the mechanical properties of PP geotextiles change with varying heavy metal concentrations after aging for 200 days at 55 °C and pH = 6. The data indicate a decrease in the tensile strength of the filament geotextiles to 19.48 MPa and 18.01 MPa, and a reduction in the elongation at break of geotextiles to 56.1% and 51.67%, in aging environments of pH = 6 (aqueous solution) and pH = 6 (heavy metal solution), respectively. Similarly, in the corresponding aging environment, the tensile strength of the staple fiber geotextiles decreased to 16.47 MPa and 15.09 MPa, respectively, and the elongation at break of the staple fiber geotextiles decreased to 78.35% and 74.90%, respectively.

Overall, the retention of mechanical properties in PP filament geotextiles and PP staple fiber geotextiles is better in aqueous solutions than in heavy metal solutions, highlighting those heavy metals catalyze the thermal oxidation of PP material at 55 °C. This suggests that the environmental tolerance of materials in heavy metal solutions is notably lower compared to those in environments without heavy metals.

Fig. 6 shows the changes in mechanical properties of PP geotextiles overtime at 55 °C and pH = 6 in a heavy metal solution. Analyze the changes in mechanical properties of PP filament geotextiles. The graph indicates a gradual decrease in tensile strength, from an initial value of 20.62 MPa–18.00 MPa over 200 days, a modest reduction of 12.7%. In contrast, the elongation at break exhibits an increasing trend, rising from 60.85% to 51.68%. This change suggests a transition from ductile to brittle behavior in the material, indicative of corrosion caused by environmental conditions leading to a slow deterioration of its mechanical properties. However, the limited extent of decline suggests resilient retention of mechanical properties during the antioxidant

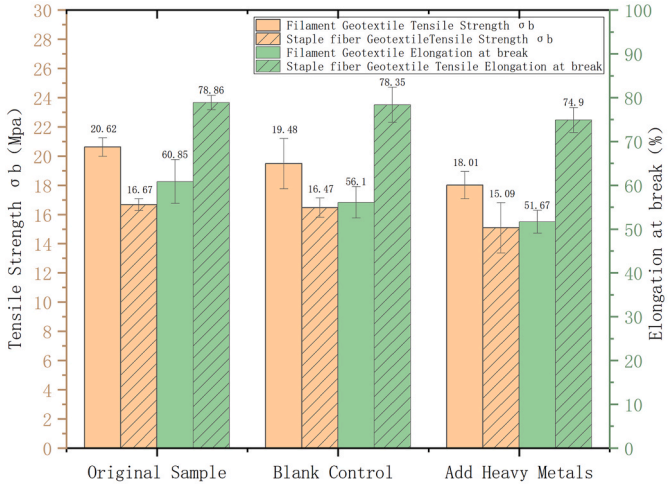

Fig. 5. Effect of heavy metal concentration on mechanical properties of PP geotextile.

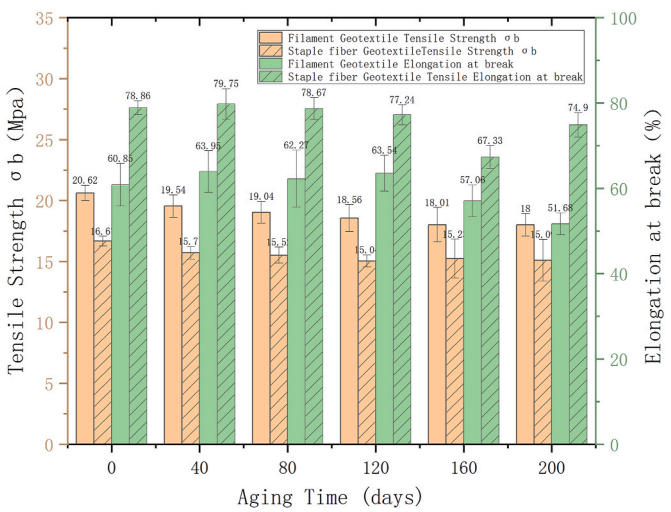

Fig. 6. Effect of exposure time on mechanical properties of PP geotextile.

consumption stage(Hsuan and Koerner, 1998; Karlsson et al., 1992). These findings underscore that prolonged environmental exposure intensifies material aging.

Analyze the changes in mechanical properties of PP short fiber geotextiles through Fig. 6. The data reveal a gradual decline in both tensile strength and elongation at break of the material. Specifically, the tensile strength dropped from an initial 16.67 MPa–15.09 MPa after 200 days, a modest decrease of 9.5%. Similarly, the elongation at break decreased from 78.86% to 74.90%. The high retention rate of the material's mechanical properties in these conditions appears to be associated with the presence of antioxidant additives. These additives are believed to interact with free radicals, alkyl peroxy radicals, and other substances generated during the aging process. They also facilitate the removal of these radicals and substances through physical processes such as migration, extraction, washing, and evaporation. This action helps maintain the mechanical properties of the geosynthetics or results in only slight declines (Karlsson et al., 1992; Rowe et al., 2010).

At 160 days into the aging test, an interesting phenomenon was observed where the tensile strength increased from 15.04 MPa to 15.23 MPa, while the elongation at break decreased from 77.24% to 67.33%. This suggests a potential "Annealing Effect" (Ferrer-Balas et al., 2001; Shi et al., 2013), wherein the intermolecular bond energy within the polymer increases, leading to increased surface tension, mitigation of internal stress and material weaknesses, and compensation of internal defects. As a result, the mechanical properties of the material are slightly enhanced. Consequently, the material transitions from a ductile to a brittle state.

3.2. Formation of microplastics

In this study, we monitored and analyzed changes in the concentration of microplastics formed from PP staple fiber geotextiles and PP filament geotextiles to assess the stability of anti-seepage materials. The results of these analyses are detailed in Fig. 7, Table 1.

Fig. 7 shows the concentration changes of microplastics formed during the aging of PP filament geotextiles. Initially, the concentration of microplastics increased from 23.67 pcs/10 mL (at 20 days) to 42.00 pcs/10 mL (at 200 days), following a non-linear trend that first decreased slowly and then increased (minimum, maximum = 21.33 pcs/10 mL, 42.00 pcs/10 mL).

During the aging of PP filament geotextiles, the MPs content first decreased from 23.67 pcs/10 mL (40 days) to 21.33 pcs/10 mL (60 days), subsequently rose to 25.33 pcs/10 mL (80 days). This fluctuation may be attributed to the "Annealing Effect" that occurred during this

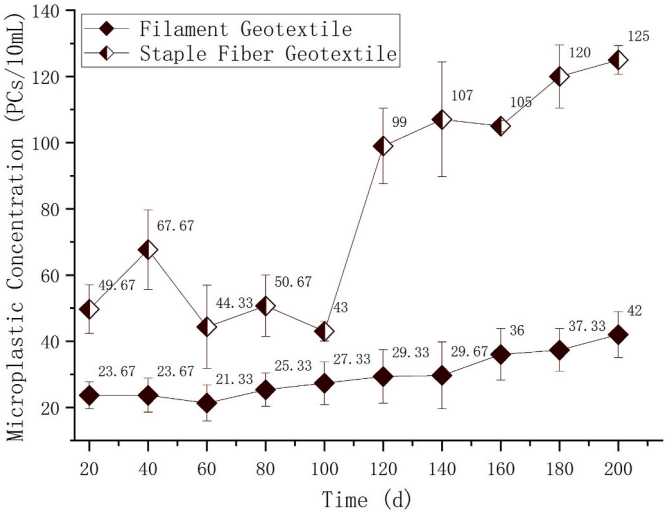

Fig. 7. Concentration variation of solution microplastics.

Table 1
Microplastic concentration of PP filament geotextile during aging.

Time (day)	Particle size			
	0.30 mm–1.00 mm (pcs/10 mL)	0.15 mm–0.30 mm(pcs/10 mL)	0.30 mm–1.00 mm (pcs/10 mL)	0.15 mm–0.30 mm (pcs/10 mL)
	Filament geotextile	Filament geotextile	Staple fiber geotextile	Staple fiber geotextile
20	8.00	15.67	29.33	20.33
40	15.33	8.33	35.33	32.33
60	9.33	12.00	21.67	22.67
80	14.33	11.00	31.00	19.67
100	14.33	13.00	20.67	22.33
120	15.33	14.00	38.33	60.67
140	15.67	14.00	46.33	60.67
160	15.67	20.33	55.00	50.00
180	15.33	22.00	59.00	61.00
200	21.00	21.00	57.33	67.67

period, which led to a reduction in the formation of large-sized microplastics (0.30 mm–1.00 mm) from 23.33 pcs/10 mL to 14.33 pcs/10 mL. Meanwhile, the formation of smaller microplastics (0.15 mm–0.30 mm) remained relatively stable (Table 1). According to the mechanical performance analysis in this study, this behavior could be linked to the reintegration of molecular chains during polymer aging, which results in increased intermolecular bond energy, surface tension, and consequently, a transformation of large-sized microplastics into smaller sizes.

Fig. 7 also indicates that the microplastic concentration of PP staple fiber geotextiles material follows a trend of initially decreasing and then increasing, with minimum and maximum values of 43.00 pcs/10 mL and 125.00 pcs/10 mL, respectively. At the beginning of the 40-day aging period, the microplastic concentration began to rise from 0 to 67.67 pcs/10 mL). Then, between 40 and 100 days, the microplastic concentration gradually decreased to 43.00 pcs/10 mL. Notably, between 100 and 120 days, the concentration surged to 99.00 pcs/10 mL, and continued to steadily increase from 120 to 200 days. These observations suggest that the material may exhibit the typical "Annealing Effect" of polymers between 40 and 120 days. Table 1 further demonstrates a significant decrease in microplastics in the 0.30 mm–0.15 mm range between 40 and 100 days compared to the larger 0.30–1.00 mm size. However, both size ranges witnessed significant increases between 100 and 120 days. This indicates that the degradation of impervious materials primarily manifests through fluctuations in the number of large-size microplastics in the early stage, and changes in the number of small-size microplastics in the middle and late stages.

Throughout the aging process of geotextiles, macromolecules continuously decompose into smaller molecules, a process mirrored in the diminishing mechanical properties of geotextiles. In conclusion, the stability of materials affected by the "Annealing Effect" during the aging process experiences a transient rise, followed by an overall decline within 120 days.

3.3. Microscopic characterization analysis

3.3.1. SEM study

Upon examining Fig. 8 (a), (b), (c), (j) and Fig. 9 (a), (b), (c), (j), it is clear that the initial surfaces of both PP filament geotextiles and PP staple fiber geotextiles are smooth and free of any marks. However, as time progresses, granular corrosion marks begin to appear on the surface, signifying a progression in material corrosion over time. Further examination of Fig. 8(a)–(e), (f), (h), (i), (g) and Fig. 9 (a), (e), (f), (h), (i), (g) reveals that corrosion under acidic and alkaline conditions is more pronounced than under neutral conditions, likely due to different concentrations of solutions retained on the material surface, leading to more severe corrosion. Additionally, an analysis of Fig. 8(a)–(d), (i), (j) and Fig. 9 (a), (d), (i), (j) highlights varying degrees of damage on the

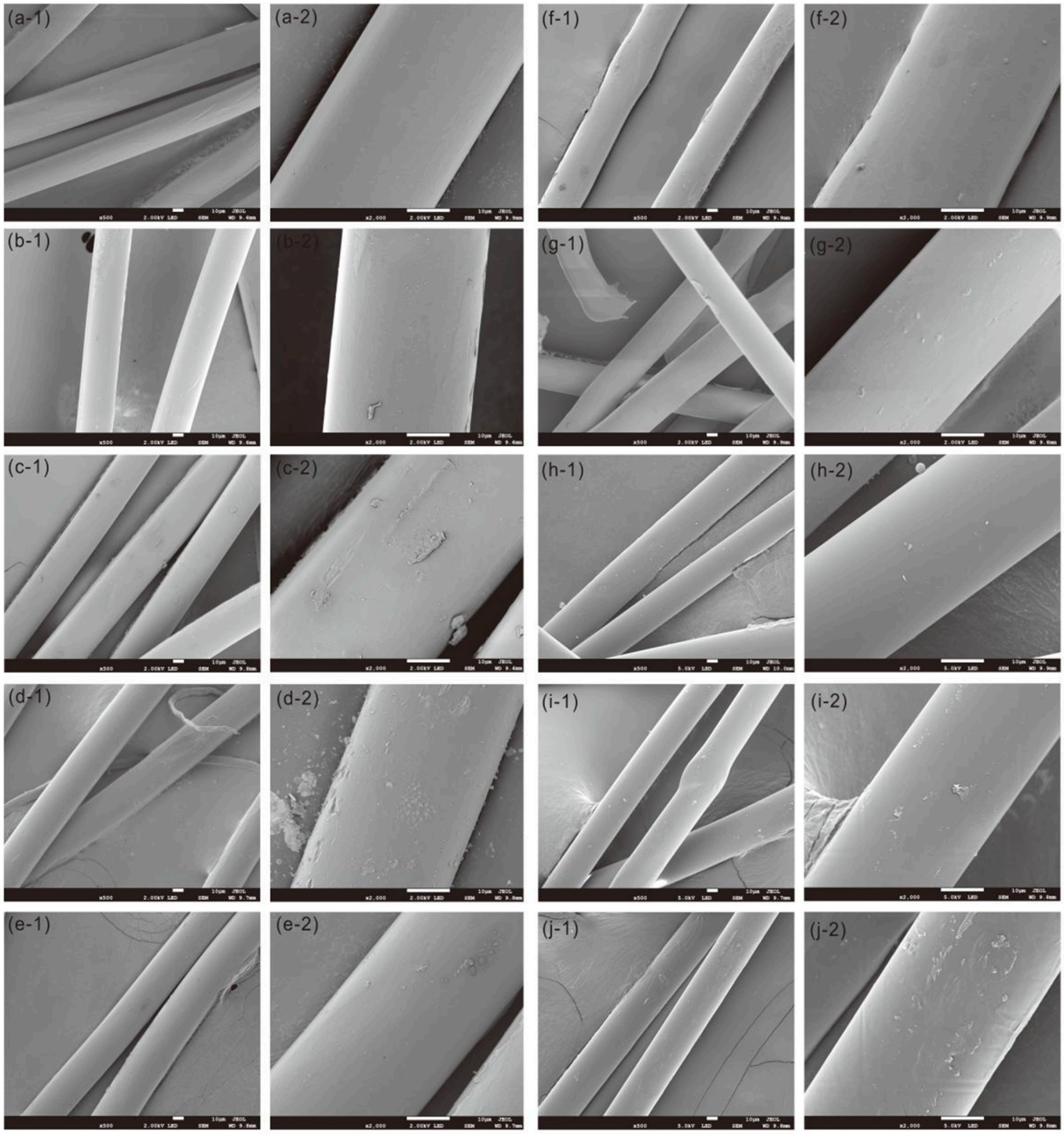

Fig. 8. SEM Images of PP filament geotextile.
Footnotes for Fig. 8:(a)original sample, (b) 40 days at 85 °C, pH = 13, (c) 80 days at 85 °C, pH = 13, (d) 200 days at 25 °C, pH = 13, (e) 200 days at 55 °C, pH = 1, (f) 200 days at 55 °C, pH = 6, (g) 200 days at 55 °C, pH = 6 (with heavy metal), (h) 200 days at 55 °C, pH = 8, (i) 200 days at 55 °C, pH = 13, (j) 200 days at 85 °C, pH = 13; where (1) represents 500x magnification, (2) represents 2000x magnification.

material surface after 200 days of aging under pH = 10 conditions. Notably, higher temperatures tend to produce larger and greater numbers of corrosion marks on the material surface, which can be attributed to surface degradation and crosslinking (Gluszewski et al., 2018). This results in reduced molecular cohesion and the formation of small detached molecules attached to the material. Concurrently, gel-like substances have been observed on the material surfaces, suggesting a potential reintegration of polymer molecular chains during the aging process as a response to repair surface damage.

3.3.2. *DSC study*

As the degradation reaction progresses, the material undergoes hydrolysis crosslinking reactions, resulting in the primary molecular chain fractures and increased degradation products. This leads to a decrease in the material's molecular weight and a reduction in melting temperature (Lu et al., 2013). The crystallinity of the aged samples was assessed using

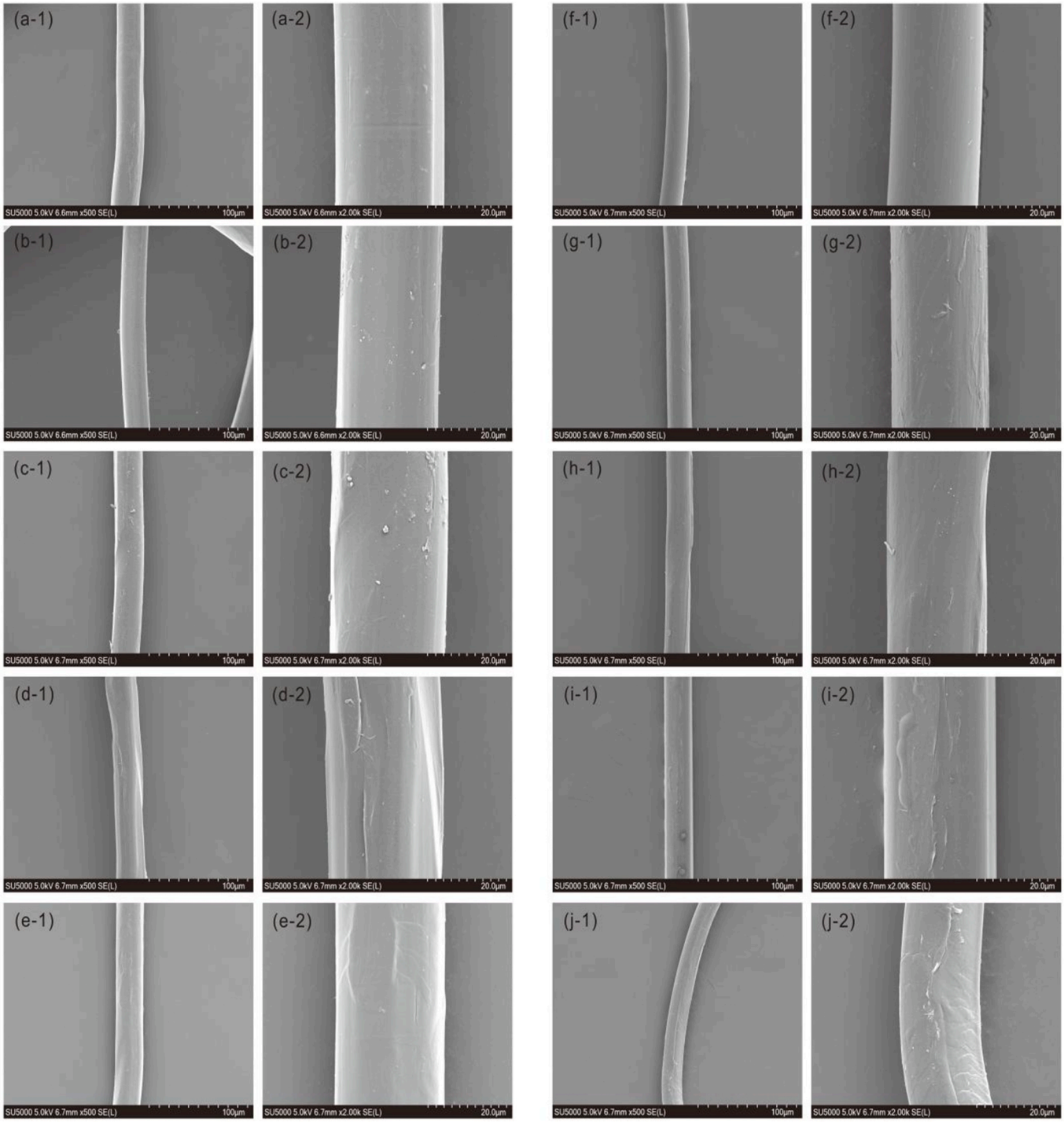

Fig. 9. SEM Images of PP staple fiber geotextile.
Footnotes for Fig. 9:(a) original sample, (b) 40 days at 85 °C, pH = 13, (c) 80 days at 85 °C, pH = 13, (d) 200 days at 25 °C, pH = 13, (e) 200 days at 55 °C, pH = 1, (f) 200 days at 55 °C, pH = 6, (g) 200 days at 55 °C, pH = 6 (with heavy metal), (h) 200 days at 55 °C, pH = 8, (i) 200 days at 55 °C, pH = 13, (j) 200 days at 85 °C, pH = 13; where (1) represents 500x magnification, (2) represents 2000x magnification.

differential scanning calorimetry (DSC), with the crystal fusion curves presented in Figs. 10 and 11. The corresponding calculated melting enthalpy of fusion values are listed in Table 2.

Differential scanning calorimetry was employed to assess the crystallinity of the aged samples, with the crystallization melting curve depicted in Fig. 10. The trend in crystallinity changes in PP staple fiber geotextiles appears consistent across different conditions, showing melting peaks falling within the range of 150 °C–180 °C. Differential scanning calorimetry was employed to assess the crystallinity of the aged samples, with the crystallization melting curve depicted in Fig. 10. The trend in crystallinity changes in PP staple fiber geotextiles appears consistent across different conditions, showing melting peaks falling within the range of 150 °C–180 °C. In Fig. 10, curve d can be seen to fluctuate significantly at about 160 °C. In this study, it is concluded that this is caused by the recrystallization phenomenon that occurs during the ageing process of the material. Due to the βα recrystallization behaviour of polypropylene during slow heating process(Lyu et al., 2023). The β-crystallites and the α-crystallites have different thermal

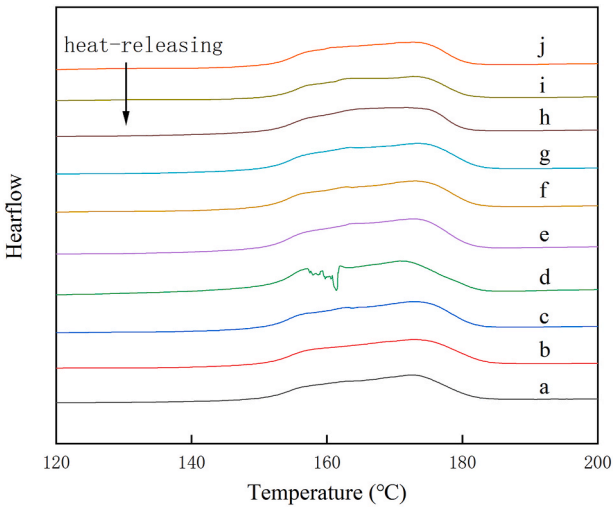

Fig. 10. DSC scans of the PP staple fiber geotextile.
Footnotes for Fig. 10: (a) original sample, (b) 40 days at 85 °C, pH = 13, (c) 80 days at 85 °C, pH = 13, (d) 200 days at 25 °C, pH = 13, (e) 200 days at 55 °C, pH = 1, (f) 200 days at 55 °C, pH = 6, (g) 200 days at 55 °C, pH = 6 (with heavy metal), (h) 200 days at 55 °C, pH = 8, (i) 200 days at 55 °C, pH = 13, (j) 200 days at 85 °C, pH = 13.

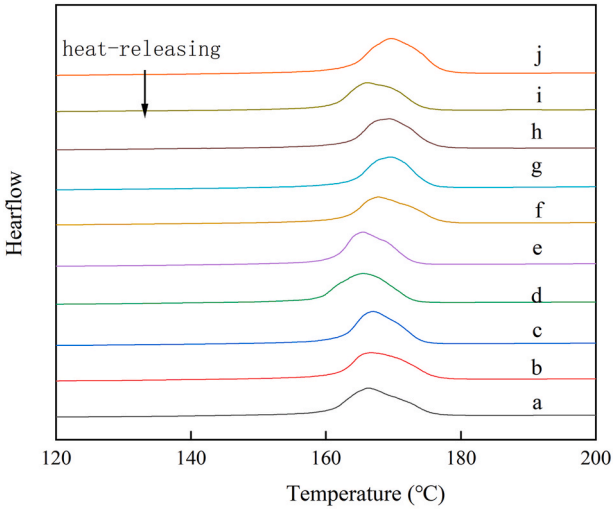

Fig. 11. DSC scans of the PP filament geotextile.
Footnotes for Fig. 11:(a) original sample, (b) 40 days at 85 °C, pH = 13, (c) 80 days at 85 °C, pH = 13, (d) 200 days at 25 °C, pH = 13, (e) 200 days at 55 °C, pH = 1, (f) 200 days at 55 °C, pH = 6, (g) 200 days at 55 °C, pH = 6 (with heavy metal), (h) 200 days at 55 °C, pH = 8, (i) 200 days at 55 °C, pH = 13, (j) 200 days at 85 °C, pH = 13.

stability, which leads to the obvious elting peak on the curve d.

Analysis from Table 2 (b), (c), and (j) reveals a decline in the melting enthalpy of the material aged for 200 days, indicative of cross-linking and decreased crystallinity (Sewda and Maiti, 2010). This decrease signifies molecular chain fracture during aging, leading to decreased molecular weight and resulting in lower melting temperatures and heat of fusion (Lu et al., 2013).

Data in Table 2 (d) indicates that when the material is aged for 200 days at 25 °C and pH = 13, it exhibits a melting peak at 160 °C and a corresponding melting enthalpy of 163.7 J/g, a significant increase from the original sample's 110.9 J/g. This suggests a potential "Annealing Effect" under this specific environmental condition (Gluszewski et al., 2018; Shi et al., 2013). Typically, polymer materials feature zones of incomplete crystallization, and annealing can promote molecular chain

Table 2
Melting enthalpy of materials under different aging conditions.

Number	PP staple fiber geotextile ΔH_m (J/g)	PP filament geotextile ΔH_m (J/g_
[a]	99.8	110.8
[b]	110.9	115.0
[c]	110.8	116.9
[d]	163.7	113.5
[e]	113.4	112.4
[f]	118.2	117.0
[g]	101.6	111.2
[h]	92.3	114.5
[i]	97.6	136.0
[j]	97.6	143.9

Footnotes for Table 2.
[a] original sample.
[b] 40 days at 85 °C, pH = 13.
[c] 80 days at 85 °C, pH = 13.
[d] 200 days at 25 °C, pH = 13.
[e] 200 days at 55 °C, pH = 1.
[f] 200 days at 55 °C, pH = 6.
[g] 200 days at 55 °C, pH = 6 (with heavy metal).
[h] 200 days at 55 °C, pH = 8.
[i] 200 days at 55 °C, pH = 13.
[j] 200 days at 85 °C, pH = 13.

reintegration, alleviating internal stress and compensating for internal defects. This process enhances mechanical properties at the macro level and increases melting enthalpy and crystallinity at the micro level.

Fig. 11 illustrates that the crystallinity of PP filament geotextiles display a similar trend under varying conditions, with melting peaks between 160 °C and 180 °C. Additionally, Fig. 11 and Table 2 (a), (b), (c), and (j) demonstrate an increase in melting enthalpy with aging (from 118.8 J/g to 143.9 J/g), suggesting an upward trend in crystallinity (Sewda and Maiti, 2010). The melting curves in Fig. 10 (e), (f), (g), (h), and (i) indicate the potential for "Rerystallization" under different aging conditions (Longxiang, 2010), particularly noting a lag or weakening of recrystallization under acidic conditions, which highlights the material's sensitivity to extreme acidity.

4. Conclusions

Based on the presented results and discussion, the following important conclusions have been drawn.

1) The increase in temperature, heavy metal concentration, and prolonged environmental exposure time will enhance the aging of geotextiles.
2) Due to varying production processes, two types of PP geotextiles demonstrated different mechanical properties. Although the PP filament geotextiles have higher initial tensile strength, it is more susceptible to accelerated aging caused by the synergistic effects of acid and high temperature during the 200-day accelerated aging process. Under neutral and alkaline conditions, both PP filament geotextiles and PP staple fiber geotextiles maintained good mechanical properties, with no significant damage observed through infrared spectroscopy analysis (Supplementary material Figures s1 and s2). The rate of tensile strength loss during aging is lower than staple fiber geotextiles.
3) The recrystallization phenomenon of geotextiles during aging slows down the loss of their mechanical properties. PP staple fiber geotextiles are more susceptible to recrystallization than filament geotextiles, which also explains why PP staple fiber geotextiles have a lower tensile strength loss rate within 200 days and exhibit more pronounced fluctuations in the amount of dissolved microplastics.

In conclusion, the research results will help to formulate a more scientific and reasonable maintenance scheme, find and deal with aging

problems in a timely manner, and extend the service life of geotechnical engineering. In the environmental remediation project, the study on the aging mechanism of heavy metals in PP geotextiles is helpful in more accurately evaluating the impact of the remediation project on the surrounding environment and selecting the appropriate remediation materials and schemes. Through the prediction and monitoring of the performance changes of PP geotextiles in a heavy metal environment, the remediation scheme is adjusted in time to reduce the adverse impact on the environment.

It has some limitations to extend this conclusion to PP geotextiles produced by other manufacturers. Because different manufacturers of PP geotextiles have different types and quantities of stabilizers, even different densities. The geotextiles are complex and changeable in the environment, and the concentration of heavy metals and pH value in the exposed environment may change to some extent. The aging characteristics of PP geotextiles in dynamic environments still need further study. In this study, the content of microplastics (MPS) dissolved in the process of material aging was quantitatively analyzed, and the smaller particle size micro-nano plastics (NPS) were not further studied. Therefore, subsequent studies can focus on the dissolution status and morphological changes of MPS and NPs in site pollution.

CRediT authorship contribution statement

Yuqi Peng: Writing – original draft, Visualization, Conceptualization. **Zongqiang Zhu:** Writing – review & editing, Funding acquisition. **Jun Zhang:** Visualization, Methodology, Data curation. **Yinian Zhu:** Supervision, Resources. **Lihao Zhang:** Supervision, Resources. **Yinming Fan:** Supervision, Resources. **Xiaobin Zhou:** Supervision, Resources. **Shen Tang:** Supervision, Resources. **Yusheng Lu:** Validation, Investigation. **Wenqian Li:** Validation, Investigation. **Yifan Xin:** Supervision, Investigation.

Declaration of competing interest

The authors declare that they have no known competing financial interests or personal relationships that could have appeared to influence the work reported in this paper.

Data availability

Data will be made available on request.

Acknowledgment

We would like to acknowledge the Guangxi Engineering Research Center of Comprehensive Treatment for Agricultural Non-Point Source Pollution and the Modern Industry College of Ecology and Environmental Protection, Guilin University of Technology for their support of this project. This work was financially supported by Guangxi Bagui Youth Talent Support Program (GuiRenCaiBan [2024]30) and the National Natural Science Foundation of China (Nos. 51978188, 42063003, 52160017, 42267027).

Appendix A. Supplementary data

Supplementary data to this article can be found online at https://doi.org/10.1016/j.geotexmem.2024.08.006.

References

Abdelaal, F.B., Rowe, R.K., Hsuan, Y.G., Awad, R., 2015. Effect of high temperatures on the physical and mechanical properties of HDPE geomembranes in air. Geosynth. Int. 22, 207–224.

Araújo, G.L.S., Sánchez, N.P., Palmeira, E.M., Almeida, M.d.G.G.d., 2022. Influence of micro and macroroughness of geomembrane surfaces on soil-geomembrane and geotextile-geomembrane interface strength. Geotext. Geomembranes 50, 751–763.

ASTM D4595-17, 2017. Standard Test Method for Tensile Properties of Geotextiles by the Wide-Width Strip Method. ASTM International, West Conshohocken, PA.

ASTM D5261-10, 2010. Standard Test Method for Measuring Mass Per Unit Area of Geotextiles. ASTM International, West Conshohocken, PA, 2010.

Bhattacharya, P., Lin, S., Turner, J.P., Ke, P.C., 2010. Physical adsorption of charged plastic nanoparticles affects algal photosynthesis. J. Phys. Chem. C 114, 16556–16561.

Browne, M.A., Galloway, T., Thompson, R., 2007. MICROPLASTIC-AN emerging contaminant of potential concern? Integrated Environ. Assess. Manag. 3, 559–561.

Carneiro, J.R., Almeida, P.J., Lopes, M.d.L., 2014. Some synergisms in the laboratory degradation of a polypropylene geotextile. Construct. Build. Mater. 73, 586–591.

Carneiro, J.R., Almeida, P.J., Lopes, M.d.L., 2019. Evaluation of the resistance of a polypropylene geotextile against ultraviolet radiation. Microsc. Microanal. 25, 196–202.

Carneiro, J.R., Lopes, M.L., 2017. Natural weathering of polypropylene geotextiles treated with different chemical stabilisers. Geosynth. Int. 24, 544–553.

Carneiro, J.R., Morais, M., Lopes, M.d.L., 2018. Degradation of polypropylene geotextiles with different chemical stabilisations in marine environments. Construct. Build. Mater. 165, 877–886.

Carneiro, J.R., Paula, A.M., Pinho-Lopes, M., 2023. Tensile behavior of weathered thermally bonded polypropylene geotextiles: analysis using constitutive models. J. Mater. Civ. Eng. 35, 04023444.

De Carvalho, A.P., Dos Santos, H.F., Ribeiro, G.D., Hiranobe, C.T., Goveia, D., Gennaro, E.M., Paim, L.L., Dos Santos, R.J., 2024. Sustainable composites: analysis of filler–rubber interaction in natural rubber–styrene–butadiene rubber/polyurethane composites using the lorenz–park method and scanning electron microscopy. Polymers 16, 471.

Ding, Z., Babar, A.A., Wang, C., Zhang, P., Wang, X., Yu, J., Ding, B., 2021. Spunbonded needle-punched nonwoven geotextiles for filtration and drainage applications: manufacturing and structural design. Compos. Commun. 25, 100481.

Dudic, D., Kostoski, D., Djokovic, V., Stojanovic, Z., 2000. Recrystallization processes induced by accelerated ageing in isotactic polypropylene of different morphologies. Polym. Degrad. Stabil. 67, 233–237.

Eskandarnia, G., Soltani, P., 2023. Effect of fabric structure on in-plane and through-plane hydraulic properties of nonwoven geotextiles. Geotext. Geomembranes 51, 1–14.

Ewais, A.M.R., Rowe, R.K., 2014. Effect of aging on the stress crack resistance of an HDPE geomembrane. Polym. Degrad. Stabil. 109, 194–208.

Ferrer-Balas, D., Maspoch, M.L., Martinez, A.B., Santana, O.O., 2001. Influence of annealing on the microstructural, tensile and fracture properties of polypropylene films. Polymer 42, 1697–1705.

Fujiyama, M., Kawamura, Y., Wakino, T., Okamoto, T., 1988. Study on rough-surface biaxially oriented polypropylene film. II. Influence of stretching conditions. J. Appl. Polym. Sci. 36, 995–1009.

Gluszewski, W., Stasiek, A., Raszkowska-Kaczor, A., Kaczor, D., 2018. Effect of polyethylene cross-linking on properties of foams. Nukleonika 63, 81–85.

Guimarães, M.G.A., de Mattos Vidal, D., de Carvalho Urashima, D., Castro, C.A.C., 2017. Degradation of polypropylene woven geotextile: tensile creep and weathering. Geosynth. Int. 24, 213–223.

Gulec, S.B., Edil, T.B., Benson, C.H., 2004. Effect of acidic mine drainage on the polymer properties of an HDPE geomembrane. Geosynth. Int. 11, 60–72.

Hsuan, Y.G., Koerner, R.M., 1998. Antioxidant depletion lifetime in high density polyethylene geomembranes. J. Geotech. Geoenviron. Eng. 124, 532–541.

Hsuan, Y.G., Li, M., Koerner, R.M., 2005. Stage "C" Lifetime Prediction of HDPE Geomembrane Using Acceleration Tests with Elevated Temperature and High Pressure. Geotechnical Special Publication, pp. 4207–4211.

Jaswal, P., Vivek, 2023a. Experimental study on monotonic behaviour of two-layered unpaved road model reinforced with treated coir geotextiles. International Journal of Pavement Research and Technology. https://doi.org/10.1007/s42947-023-00293-z.

Jaswal, P., XXX, V., Sinha, S.K., 2022. Investigation on tensile strength characterisation of untreated and surface treated coir geotextiles. J. Ind. Textil. 52, 15280837221118847.

Ji, B., Qi, H., Yan, K., Sun, G., 2016. Catalytic actions of alkaline salts in reactions between 1,2,3,4-butanetetracarboxylic acid and cellulose: I. Anhydride formation. Cellulose 23, 259–267.

Karademir, T., Frost, J.D., 2014. Micro-scale tensile properties of single geotextile polypropylene filaments at elevated temperatures. Geotext. Geomembranes 42, 201–213.

Karademir, T., Frost, J.D., 2021. Elevated temperature effects on geotextile–geomembrane interface shear behavior. J. Geotech. Geoenviron. Eng. 147, 04021148.

Karlsson, K., Smith, G.D., Gedde, U.W., 1992. MOLECULAR-STRUCTURE, morphology, and antioxidant consumption in medium density polyethylene pipes in hot-water applications. Polym. Eng. Sci. 32, 649–657.

Kurniawan, S.B., Said, N.S.M., Imron, M.F., Abdullah, S.R.S., 2021. Microplastic pollution in the environment: insights into emerging sources and potential threats. Environmental Technology & Innovation 23.

Liu, X., Liu, H.Y., Li, Y.F., Zhao, J.H., Yang, R., 2020. Infectious effect of organic small molecules on photo-oxidative aging of polypropylene. Chemical Journal of Chinese Universities-Chinese 41, 2838–2844.

Liu, X., Yang, R., 2020. Conversion among photo-oxidative products of polypropylene in solid, liquid and gaseous states. Bmc Chemistry 14.

Long, X., He, L., Zhang, Y., Ge, M., 2018. Multicomponent composite emulsion treated geotextile on landfill with improved long-term stability and security. Journal of Engineered Fibers and Fabrics 13, 155892501801300307.

Longxiang, T., 2010. Reasons for Thermochromism of PP/Elastomer Alloys. Modern Plastics Processing and Applications.
Lu, W.M., Li, N., Yuan, Z.L., Ding, X.M., 2013. Photodegradation performance and evaluation methods of non-durable non-woven fabrics. Adv. Mater. Res. 2735.
Lyu, D., Chen, R., Lu, Y., Men, Y., 2023. Mechanism of βα recrystallization in isotactic polypropylene. Polymer 279, 126011.
Meides, N., Mauel, A., Menzel, T., Altstädt, V., Ruckdäschel, H., Senker, J., Strohriegl, P., 2022. Quantifying the fragmentation of polypropylene upon exposure to accelerated weathering. Microplastics and Nanoplastics 2, 23.
Nisar, J., Shafi, Mir M., Vivek, 2023. Study on optimal preparation and rheological characteristics of waste low density polyethylene (LDPE)/styrene butadiene styrene (SBS) composite modified asphalt binder. Construct. Build. Mater. 407, 133459.
Osawa, Z., Ishizuka, T., 1973. Catalytic action of metal salts in autoxidation and polymerization. X. The effect of various metal stearates on the thermal oxidation of 2,6,10,14-tetramethylpentadecane. J. Appl. Polym. Sci. 17, 2897–2907.
Philipp, S., Ieva, P., Ieva, B., Ineta, L., Evita, S., Alexandr, K., Elena, E., Boris, C., Ingrida, P., FranzGeorg, S., 2021. Environmental impact of geosynthetics in coastal protection. Materials 14.
Rowe, R.K., Asce, F., Islam, M.Z., Hsuan, Y.G., 2010. Effects of thickness on the aging of HDPE geomembranes. J. Geotech. Geoenviron. Eng. 136, 299–309.
Santos, E.C.G., Palmeira, E.M., Bathurst, R.J., 2014. Performance of two geosynthetic reinforced walls with recycled construction waste backfill and constructed on collapsible ground. Geosynth. Int. 21, 256–269.
Scanferla, P., Calgaro, L., Quaresmini, R., Zambon, M., Pellay, R., Ferrari, G., Marcomini, A., 2023. The validation of converting pyrite ash-contaminated soil into End-of-Waste by the High-Performance Solidification/Stabilization process application. Integrated Environ. Assess. Manag. 19, 961–969.
Scholz, P., Falkenhagen, J., Wachtendorf, V., Brüll, R., Simon, F.-G., 2024. Investigation on the durability of a polypropylene geotextile under artificial aging scenarios. Sustainability 16, 3559.
Sedlář, J., Pác, J., 1974. Polypropylene stability adversely affected by volatile oxidation products. Polymer 15, 613–614.
Sewda, K., Maiti, S.N., 2010. Crystallization and melting behavior of HDPE in HDPE/teak wood flour composites and their correlation with mechanical properties. J. Appl. Polym. Sci. 118, 2264–2275.
Shi, S., Pan, Y., Lu, B., Zheng, G., Liu, C., Dai, K., Shen, C., 2013. Realizing the simultaneously improved toughness and strength of ultra-thin LLDPE parts through annealing. Polymer 54, 6843–6852.
Sprague, C.J., Sprague, J.E., 2016. 24 - geosynthetics in erosion and sediment control. In: Koerner, R.M. (Ed.), Geotextiles. Woodhead Publishing, pp. 531–562.
Thompson, R.C., Olsen, Y., Mitchell, R.P., Davis, A., Rowland, S.J., John, A.W.G., McGonigle, D., Russell, A.E., 2004. Lost at sea: where is all the plastic? Science 304, 838, 838.
Tollner, E.W., Annis, P.A., Das, K.C., 2011. Evaluation of strength properties of polypropylene-based polymers in simulated landfill and oven conditions. J. Environ. Eng. 137, 291–296.
Vivek, 2023. Effects of cyclic loading on sand overlaying clay model of unpaved roads reinforced with untreated/treated coir geotextiles. J. Text. Inst. 1–7.
Vivek, Dutta, R.K., 2022. Bearing ratio behavior of sand overlying clay with treated coir geotextiles at the interface. J. Nat. Fibers 19, 7534–7541.
Vivek, Dutta, R.K., Kumari, A., 2022a. Effect of chemical treatment on the durability behavior of coir geotextiles. J. Nat. Fibers 19, 3127–3146.
Vivek, Dutta, R.K., Parti, R., 2019. Effect of chemical treatment of the coir geotextiles on the interface properties of sand–/clay–coir geotextile interface. J. Inst. Eng.: Series A 100, 357–365.
Vivek, Dutta, R.K., Parti, R., 2020. Effect of chemical treatment on the tensile strength behavior of coir geotextiles. J. Nat. Fibers 17, 542–556.
Vivek, Shafi, Mir, M., Sehgal, R., 2022b. Studies of modulus of resilience on unpaved roads reinforced with untreated/treated coir geotextiles. J. Nat. Fibers 19, 13563–13573.
Vivek, Shafi, Mir, M., Sehgal, R., 2022c. Study on bearing capacity of unpaved roads reinforced with coir geotextiles using finite element method (fem). J. Nat. Fibers 19, 11735–11748.
Xu, W., Huang, W., Cai, Y., Tao, J., 2021. Classification of geotextiles and analysis on tests for their tensile properties. J. Phys. Conf. 2009, 012012.
Xu, Y.H., Ou, Q., van der Hoek, J.P., Liu, G., Lompe, K.M., 2024. Photo-oxidation of micro- and nanoplastics: physical, chemical, and biological effects in environments. Environmental Science & Technology 58, 991–1009.
Yu, Y., Ding, Y., Miao, C., Yang, X., Ge, S., 2024. Exploring the influence of sludge dewatering agents on Microplastic aging under hydrothermal treatment: insights from Polylactic Acid microplastics. Environ. Res. 240.
Zhang, F., Cao, Y., Liu, X., Xu, H., Lu, D., Yang, R., 2021. How small molecules affect the thermo-oxidative aging mechanism of polypropylene: a reactive molecular dynamics study. Polymers 13, 1243.
Zhou, S.-J., Du, Y.-J., Sun, H.-Y., Yuan, H., Feng, Y.-S., Xia, W.-Y., 2022. Evaluation of the effectiveness of ex-situ stabilization for arsenic and antimony contaminated soil: short-term and long-term leaching characteristics. Sci. Total Environ. 848.
Jaswal, P., Vivek, Sinha, S.K., 2023. Laboratory analysis of the interface shear characteristics of chemically treated coir geotextiles and soil interface. Int. J. Pavement Res. Technol. https://doi.org/10.1007/s42947-023-00369-w.
Vivek, Jaswal, P., 2024. Evaluation of untreated and treated coir geotextile performance under cyclic loading on unpaved roads. Int. J. Pavement Res. Technol. https://doi.org/10.1007/s42947-024-00430-2.